Lattice vibrations in $La(Ce)Fe_4Sb_{12}$ and $CoSb_3$: Inelastic neutron scattering and theory

J. L. Feldman
Center for Computational Materials Science, Naval Research Laboratory, Washington, DC 20375, USA

Pengcheng Dai and T. Enck
Department of Physics and Astronomy, The University of Tennessee, Knoxville, Tennessee 37996-1200, USA and Center for Neutron Scattering, Oak Ridge National Laboratory, Oak Ridge, Tennessee 37831-6393, USA

B. C. Sales, D. Mandrus, and D. J. Singh
Condensed Matter Sciences Division, Oak Ridge National Laboratory, Oak Ridge, Tennessee 37831-6032, USA
(Received 24 August 2005; revised manuscript received 12 October 2005; published 27 January 2006)

We present results of time-of-flight inelastic neutron scattering phonon density of states measurements on $(La,Ce)_{0.9}Fe_4Sb_{12}$ and $CoSb_3$ as well as of a detailed comparison with lattice dynamical models in the literature. The MARI experimental setup is replicated by a theory for scattering from a polycrystalline material. The model considered for the filled materials is a local density approximation (LDA) based short-range force constant model and those considered for $CoSb_3$ are the LDA-based model with the La-related parameters removed and a semiempirical model. We show that the presence of La significantly affects the shape of the spectrum. We also conclude that upon filling the Sb intrasquare force constants are weakened and that the transition-metal Sb bonds are almost unchanged.

DOI: 10.1103/PhysRevB.73.014306 PACS number(s): 63.20.Pw, 63.20.Dj, 78.70.Nx

I. INTRODUCTION

The rattling ion proposal by Slack[1] has been a focus of studies of promising thermoelectric materials and especially the filled skutterudites. The thermoelectric figure of merit depends inversely on the thermal conductivity, and it is desirable to achieve as small a lattice contribution to the thermal conductivity as is feasible. Fundamentally, the skutterudites typically consist of transition metal (TM) atoms on a simple cubic sublattice and pnicogen atoms in nearly square, rectangular, rings within $\frac{3}{4}$ of the cubes defined by the TM atoms. Pnicogen atoms in adjacent cubes form cages that may either be filled or empty. The Slack proposal was that introducing ions into the cages of the binary skutterudites would decrease their thermal conductivity by virtue of a rattling ion scattering of phonons.[1] These *filled* skutterudites—typically filled with rare earth ions—have the same (cubic) crystallographic space group as the binary ones. Indeed, upon investigation of the filled skutterudites a factor of 5 lower thermal conductivity than that of the binaries was obtained and therefore much attention has been paid to the dynamics of the rattling ion. In addition to infrared absorption measurements,[2] which are sensitive to zone center modes, there have been three different spectroscopic studies manifesting the rattling ion contribution to the vibrational frequency spectrum.[3–5] The Slack conjecture has been extremely fruitful, not only for skutterudites but for clathrates as well. However, the simple physical scenario of a strongly anharmonically vibrating "rattling ion" does not apply to the skutterudites. For the skutterudites, through both analyses of experimental data and first principles calculations,[6] the rattling ion vibration has been observed to have a fundamentally harmonic character. On the other hand, large mean square atomic displacements of the filler atoms are characteristic of the filled skutterudites,[7] which suggests that anharmonic scattering of phonons by the filler atoms might be important. A rigorous calculation of thermal conductivity is a difficult task and there are few such calculations for any material. As a precursor to such a calculation, it is essential to have a good description of the lattice dynamics. The lattice dynamics of the skutterudites is also intrinsically interesting, as the crystal structure is unusual and there is a richness in the nature of the vibrational modes.

For the lanthanum antimonide skutterudites, the purest materials that have been obtained contain about 10% lanthanum vacancies. In this work, we present inelastic neutron scattering (INS) measurements of phonon density of states for $La_{0.9}Fe_4Sb_{12}$, $Ce_{0.9}Fe_4Sb_{12}$, and $CoSb_3$ and we compare them with lattice dynamical models.[8,9] The models were based, at least partially, on local density approximation (LDA) first principles results and involve only short-range force constants. The comparisons test the models and also allow us to draw conclusions about the relation of force constants between filled and unfilled materials, as well as about the effects of particular force constants on the neutron spectra. We also provide dispersion curves (in an Appendix) and contributions to the vibrational density of states (VDOS) based on the models.

While we were in the process of preparing the present manuscript, a different study of the inelastic neutron spectrum of the lanthanum and cerium filled materials based on time-of-flight measurement at the IN4 spectrometer of the Institut Laue-Langevin (ILL) has appeared.[10] Since the ILL measurements were taken with incident neutron energy of 50 meV, our time-of-flight measurements at the MARI spectrometer of the Rutherford-Appleton Laboratory using incident energies of both 30 and 50 meV have provided somewhat larger dynamic range and allowed the determination of the energy dependence of the inelastic spectra. In addition, the comparison between theory and experiment given in our paper allows us to determine directly the force constants responsible for the observed phonon spectra.

The paper is organized as follows: Sec. II contains the experimental details, Sec. III the experimental results, Sec. IV the expressions used for replicating the experiment and other theoretical details, Sec. V the comparison between theory and experiment, Sec. VI plots of atomic specie contributions to the INS spectra, Sec. VII plots of VDOS contributions, Sec. VIII a comparison with optical data, Sec. IX a data reanalysis for extracting possible rattling ion contributions to the VDOS, and Sec. X the conclusions. The Appendix contains plots of dispersion curves.

II. EXPERIMENTS

We performed time-of-flight inelastic neutron scattering measurements at $T=20$ K on powder samples of $La_{0.9}Fe_4Sb_{12}$, $Ce_{0.9}Fe_4Sb_{12}$ and $CoSb_3$ of approximate masses of 30, 30, and 60 g, respectively. The experiments were performed using the MARI chopper spectrometer at the ISIS facility, Rutherford Appleton Laboratory, U.K., as described before.[11] The detectors on MARI cover a wide scattering angle from 3° to 135° and are ideal for phonon density of states measurements. For the experiments, we use incident neutrons of energies 30 and 50 meV. The Fermi chopper speed for the experiment was set to 250 Hz. The powder samples were mounted inside an aluminum sample can mounted on the cold head of a helium closed-cycle refrigerator. A preliminary report based on these measurements[3] provided the first observation of a low frequency rattling ion vibration in a filled skutterudite. In examining Q cuts (cuts with different integrations of momentum transfers) of the data, the aluminum-can contribution and a small energy-independent background contribution to $(k_0/k)(d^2\sigma/d\Omega dE)$ have been subracted out, where k and k_0 are the scattered and initial neutron momenta, respectively, E is the scattered neutron energy, and Ω is the solid angle of scattering. The background contribution was chosen such that the scattering intensity is zero for energy transfers beyond the maximum phonon energy in the case of 50 meV incident neutrons and beyond the Raman spectral region in the case of 30 meV incident neutron energy. No effort was made to subtract out the low energy elastic line and therefore evidence of the elastic contribution is seen in the results presented. What is plotted is (symbolically, as Q cuts are taken)

$$I = \frac{k_0}{k}\epsilon\frac{d^2\sigma}{d\Omega dE},$$

where the energy transfer is ϵ, as this closely corresponds to to the "neutron weighted" VDOS.

III. INELASTIC NEUTRON SCATTERING RESULTS

The experimental results for $E_i=30$ meV are given in Fig. 1, where the 5–7 Å^{-1} cuts are shown, and, for $E_i=50$ meV, a comparison of Q cuts is given in Fig. 2. The spectral shapes depend on the incident neutron energy because of energy-resolution effects. The energy resolution varies as a function of both incident energy and energy transfer, with best resolution at highest energy transfer and smallest incident energy. On the other hand, since the averaging area

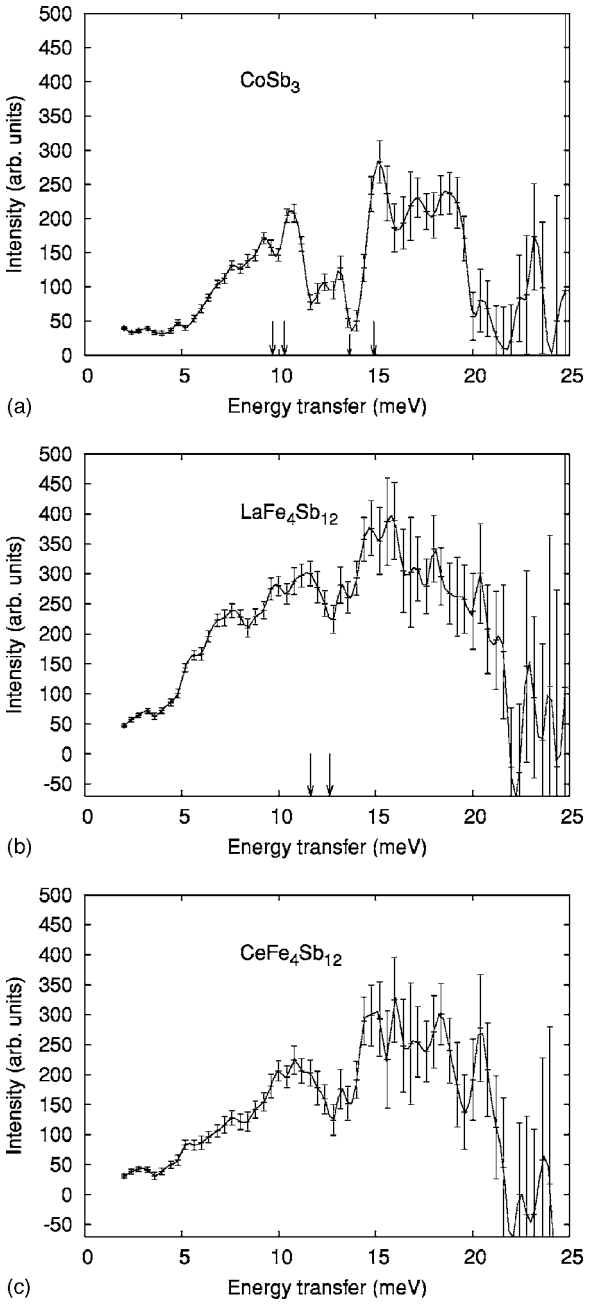

FIG. 1. INS results ($E_i=30$ meV, $Q=5-7$ Å^{-1}) for $CoSb_3$ and $La(Ce)_{0.9}Fe_4Sb_{12}$. In the case of $CoSb_3$ the arrows correspond to the pairs of infrared and Raman modes (F_g) of lowest frequencies, where the infrared modes are the outermost ones. In the case of $La_{0.9}Fe_4Sb_{12}$ the two lowest frequency Raman modes are shown and they are also of F_g symmetry.

$(\Delta Q\,\delta\epsilon)$ for a Q cut goes to zero as the incident energy is approached, the uncertainty in the Q-cut intensity increases with increasing energy transfer.

Whereas some of the broad features of these spectra, particularly the broad two-peak characteristics below 20 meV, were observed before in INS experiments,[12] the fine structure in these spectra has not been previously reported. Shown in Fig. 1 are the experimental results for the lowest frequency Raman (F_g)[9,13] and IR (F_u)[14] modes, where the latter are

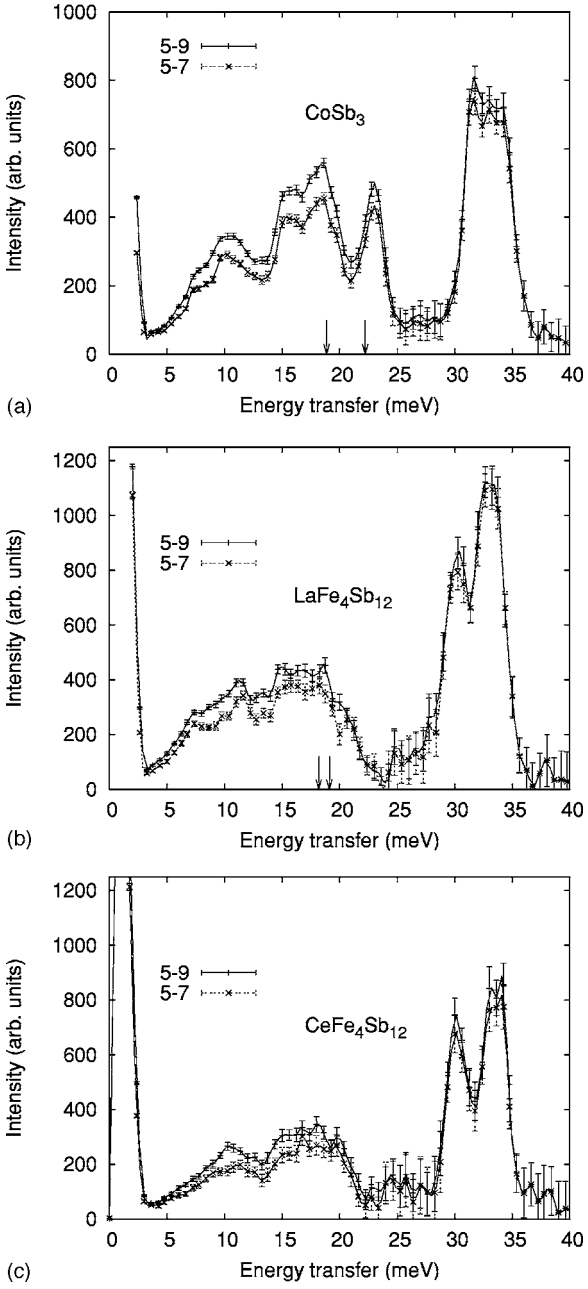

FIG. 2. INS results (E_i=50 meV) for $La(Ce)_{0.9}Fe_4Sb_{12}$ and $CoSb_3$. Both 5–7 Å^{-1} and 5–9 Å^{-1} Q cuts are shown. The arrows correspond to experimental Raman A_g frequencies.

known only for $CoSb_3$ and they bracket the Raman lines. These optical data are clearly consistent with the narrower valleys (in the 10–15 meV region) in the neutron spectra for the filled materials than for the unfilled material. We also remark that the two weak peaks in the INS spectrum of $CoSb_3$ below 10 meV, seen only in the 30 meV incident energy data, do not match any optical modes and are most likely Brillouin-zone boundary related (see Appendix). Finally, the rattling ion vibration is observed as the peak at about 7 meV in the $LaFe_4Sb_{12}$ results: The observed effect in the $CeFe_4Sb_{12}$ results at the same frequency is small because of the relatively small Ce atomic cross section.[3]

We compare the results for E_i=50 meV with the Raman measured A_g frequencies. The two A_g modes roughly correspond to areal and areal-conserving Sb-ring distortions, and the LDA results indicate that the lower frequency is the areal-conserving one. Again, the separation between optic mode frequencies correlates with the neutron spectral features, and $CoSb_3$ has more widely separated Raman frequencies and features in the neutron spectrum than do the filled materials. Nuclear inelastic scattering on $EuFe_4^{57}Sb_{12}$ and $CeFe_4^{57}Sb_{12}$ unambiguously identifies the high frequency split peaks of the filled materials as Fe-atom vibrations.[5] The data show peaks in approximately the same region of frequencies for all three materials, but the peaks are not split in the case of $CoSb_3$. It also appears that the splitting is greater in the case of the Ce-filled sample than in the case of the La-filled sample.

Finally, whereas the quantities under consideration in this paper are primarily governed by the VDOS and are therefore consistent with results based on incoherent scatterers, we have also observed coherent scattering effects. Such effects appear as oscillations, with respect to Q, in ϵ cuts and are present because La, Fe, and Sb have predominantly coherent atomic cross sections.

IV. BASIC THEORY FOR MIMICKING MARI INELASTIC NEUTRON SCATTERING RESULTS AND APPROXIMATIONS

We have followed the work of Bredov *et al.*[15] on expressions for INS from a polycrystalline solid and in the coherent scattering regime. We implemented them using a computer code that we developed. The appropriate generalization of the expressions obtained by Bredov *et al.*, which were for a Bravais crystal, is straightforward,

$$\frac{d^2\sigma_{coh}}{d\Omega dE} = \frac{\hbar}{8\pi}\frac{k}{k_0}\sum_s \int d\mathbf{q}\,\delta[\epsilon - \hbar\omega(s,\mathbf{q})]\frac{n_{s,\mathbf{q}}+1}{\omega(s,\mathbf{q})} \times \sum_\tau {\int}' dQ\,\delta(Q - |\mathbf{q}-2\pi\tau|)F_s^{\mathbf{q}-2\pi\tau}(\mathbf{q})p(|\mathbf{q}-2\pi\tau|). \quad (1)$$

Here the structure factor is defined as

$$F_s^{q-2\pi\tau}(\mathbf{q}) = \left| \sum_i a_{i,coh} e^{-W_i(Q)} e^{i(\mathbf{q}-2\pi\tau)\cdot\mathbf{R}_i} \frac{e_i^{\mathbf{q}-2\pi\tau}(s,\mathbf{q})}{\sqrt{M_i}} \right|^2.$$

In these expressions the notation chiefly combines that of Bredov *et al.*[15] and of Eschrig *et al.*[16] For our data analysis we find that $p(Q)$ should be taken as the inverse of the range of Q for which neutrons are scattered, a function of energy transfer, and also restricted by the limiting scattering angles of the MARI setup as well as by the chosen Q cut; the prime on the integral over Q denotes that the integral is performed over a similarly restricted range. The expression is also averaged over small energy bins; the energy-dependent Dirac delta function of the expression picks out the relevant normal modes. Note that these expressions are for phonon creation, corresponding to the present experiments, opposite to what Bredov *et al.* considered.

The required normal mode frequencies and polarization vectors were obtained from existing force constant models. For both La- and Ce-filled materials the LDA-based short-range model of Ref. 9 for $LaFe_4Sb_{12}$ was employed. For $CoSb_{12}$ the Born-von Karman (BvK) model *C* of Ref. 8 and a "skeletal" LDA-based model[9] were both employed. These models will be discussed in more detail in the following section. We have also calculated[19] the mean square displacements (MSD) as a function of temperature for our LDA model of $LaFe_4Sb_{12}$ and used the same set of Debye-Waller factors (DW) factors (evaluated at $T=20$ K) for $CoSb_3$, $LaFe_4Sb_{12}$, and $CeFe_4Sb_{12}$ since the DW effect in the intensity is only several percent. The theory of Bredov *et al.* also requires the use of only the isotropic values of MSDs. In evaluating the expressions for the intensity we made use of cubic grids of both 145 and 1450 points in the irreducible element (1/24th) of the Brillouin zone. The larger grid size was adequate for obtaining the theoretical INS results, as there were either small or negligible effects of using the smaller grid.

The expression for coherent scattering includes that for incoherent scattering, and for sufficiently large Q cuts, i.e., for volumes in reciprocal space significantly larger than that of the first Brillouin zone, the differences in results from the expression for incoherent scattering are expected to vanish.[17] We have performed calculations with expressions for both coherent and incoherent scattering and have found that for the selected Q cuts of this paper the incoherent approximation is valid. The validity of the incoherent approximation allows for an admittedly overly simplified approximation for the effect of partial filling; we approximate the rare earth contribution to be 90% of the perfect crystalline value. It also allows for a uniform treatment of both coherent and incoherent scattering contributions.

The results of the above expression must be convoluted with the instrumental resolution function in order to compare with experiment. The resolution function is a Gaussian, for the conditions of this experiment, with an energy-dependent full width at half maximum (FWHM) that depends on the Fermi chopper speed. (We shall refer to this as the theoretical instrumental broadening function.) Finally, although we make use of scaling factors to compare intensities with experiment, we use arbitrary values only between results for different materials and between results for different incident neutron energies. Therefore, where we show multiple results for a given incident energy and material, the results correspond to the same scaling.

V. COMPARISONS BETWEEN THEORY AND EXPERIMENT FOR INS SPECTRA

In this section we show the comparisons between theory and experiment, where, as discussed above, we employ both our LDA-based model and a Born-von Karman model. The LDA model was obtained for $LaFe_4Sb_{12}$ and was derived by choosing zone centerlike displacements and cutting the force constants off. In the case of $CoSb_3$, we consider two models.

TABLE I. Force constant, $-\Phi_{\alpha\beta}(i,j)(10^4$ dyn/cm)

Atoms/$\alpha\beta$	filled	unfilled
3,3		
xx	−17.2(2)	−17.6
xy	1.6(2)	0.8
11,11		
xx	−15.1(3)	15.2
yy	−10.4(1)	−8.92
zz	−11.7(2)	−11.6
yz	0.2(2)	1.4
11,15		
yz	0.03(15)	−0.49
$1,11'$		
yz	0.23(18)	0.01

One model (model 1) is obtained by removing effects of La on the force constants for $LaFe_4Sb_{12}$ as described in our earlier paper[9] and the other model (model 2) is based on a Born-von Karman fit to both the measured infrared frequencies and LDA theoretical results for the A_g and A_u modes (model *C* of Ref. 8). We elaborate on model 1 as it has not been discussed in any detail. The results given for force constants in our previous paper are least square fitted values where restrictions on the force constants, due to conservative forces and rigid translational symmetry, are imposed as constraints. Therefore, removal of lanthanum implies a change in the self-force-constants since the self-force-constants $[\Phi(i,i)]$ are expressed in terms of sums over the pair-force-constants $[\Phi(i,j)]$ by virtue of rigid translational symmetry. Furthermore a change in two pair-force-constants occurs as a result of the requirement that self-force-constant matrices must be symmetric by virtue of the conservative force requirement. We show the relevant force constants in Table I. Values in parenthesis are the least squares uncertainties. We refer the reader to Ref. 9 for the structural labels.

A. $E_i=30$ meV

We find that upon applying Gaussian broadening to our model results for the INS intensities, the best fit to the experimental results for $LaFe_4Sb_{12}$ in the rattling ion (7 meV) spectral region corresponds to a Gaussian broadening parameter FWHM$\approx$2.1 meV. However, the theoretical instrumental energy resolution, which varies monotonically from FWHM$\approx$0.9 meV at $\epsilon=0$ to FWHM$\approx$0.3 meV at $\epsilon=30$ meV (for the 250 Hz Fermi chopper speed of the experiment), is approximately FWHM$\approx$0.75 meV at $\epsilon\approx7$ meV.[18] In addition to the limitation of energy resolution based solely on Fermi chopper speed, perhaps other instrumental uncertainties as well as structural disorder broadens the experimental peak at 7 meV. In order to achieve a broadening of 2.1 meV in the rattling ion spectral region we require an *additional* Gaussian broadening of FWHM =2 meV. Figure 3 gives comparisons of the data with broadened theoretical results over a wide energy range consistent

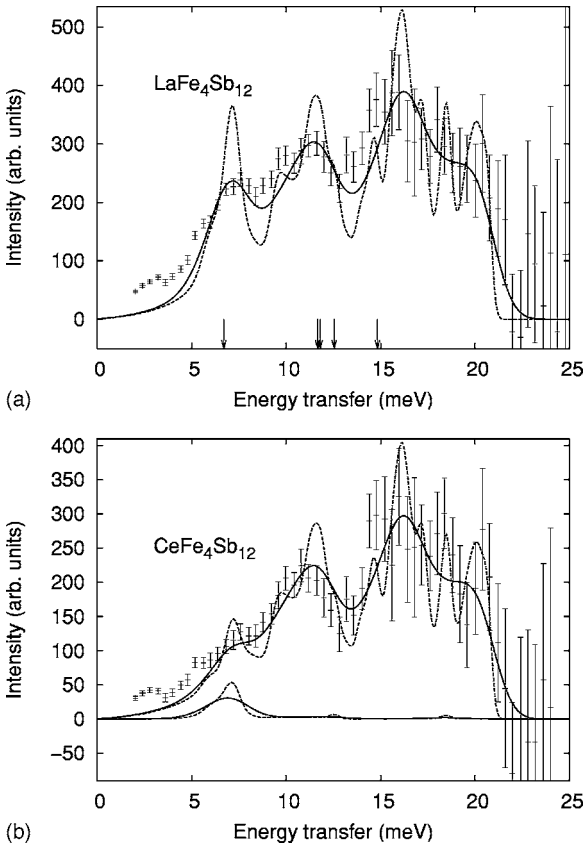

FIG. 3. INS and model results. Results indicate possible effect of disorder. In one calculation (dashed line) the theoretical instrumental broadening, $\Delta_{ins}(E)$, is applied to the model and in the other calculation (solid line) $\Delta(E)=\sqrt{[2^2+\Delta_{ins}(E)^2]}$ is used for the broadening (FWHM). The arrows correspond to the lowest frequency calculated infrared and Raman (F_g) modes. The lowest frequency optical mode is infrared active and the two outermost modes (among the modes above 10 meV) are infrared active. The Ce contribution to the spectrum for $Ce_{0.9}Fe_4Sb_{12}$ is also given.

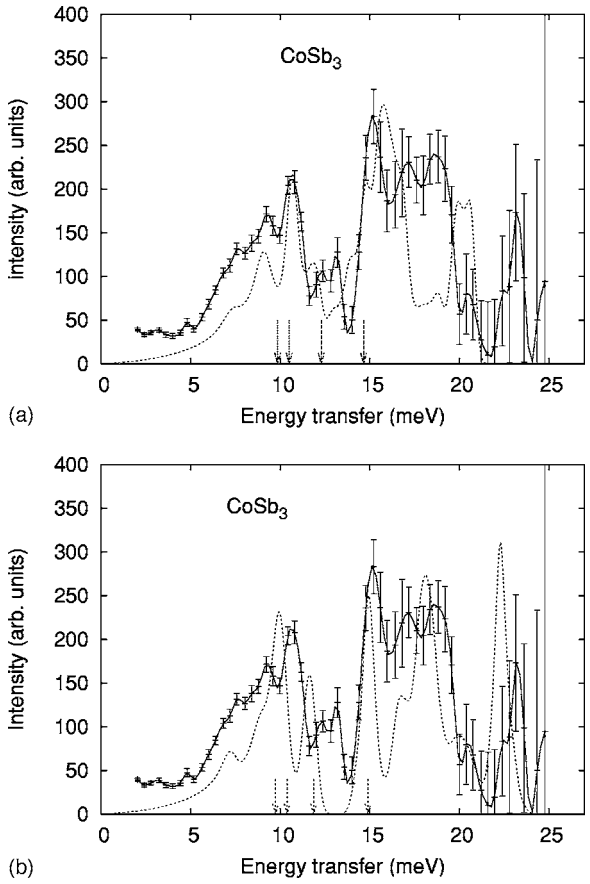

FIG. 4. INS results for $CoSb_3$ and corresponding results for models 1 (upper panel) and 2 (lower panel) (see text). The arrows correspond to the calculated lowest frequency pairs of Raman and infrared modes, where the outer modes are infrared.

with $E_i=30$ meV. If the added broadening were solely due to structural disorder, then we would have evidence of Anderson-like localized modes,[20] or perhaps of independent resonance modes, since the spectrum in the 7 meV region is continuous; in this case, the structural-disorder broadening would be comparable to the width of the corresponding peak in the calculated VDOS of the perfect crystal (see Ref. 9 and a later figure). We stress that the above observations rely on the validity of the LDA-based model.

Our results for $CoSb_3$ (see Fig. 4) provide an interesting comparison because they show that for a system not expected to have significant structural disorder the theoretical instrumental broadening yields satisfactory results.

B. $E_i=50$ meV

In order to directly compare theory and experiment over a wide range of energy transfers using MARI, it can be instructive to use a scissors approximation, whereby separated regions of the spectra are matched, according to energy transfer, between theory and experiment. This is because of the kinematics associated with the experiment. For a given incident energy the allowed range of momentum transfer to the lattice, in the one phonon regime, varies monotonically from zero at total energy transfer to $2k_i$ at zero energy transfer. Therefore the averaging area in Q-E space for a given Q cut depends on the region of the spectrum under consideration and it is clear, taking into account the Q^2 dependence of the intensity at fixed energy transfer, that when one has a gap in the phonon spectrum the best comparison between theory and experiment (for the relative intensities of the two regions) is achieved with use of a scissors approximation. We show this for $LaFe_4Sb_{12}$ in Fig. 5. In this approximation for $LaFe_4Sb_{12}$, the mode frequencies above 25 meV within the lower and higher frequency bands (see Ref. 9 and a later figure) have been shifted upward by 2.7 meV and 2.2 meV, respectively. The calculation is also based on the so-called "disorder" broadening. As previously defined, disorder broadening corresponds to a 2 meV broad Gaussian function convoluted with the theoretical resolution function. For $E_i=50$ meV the theoretical instrumental broadening function is a Gaussian with broadening parameter (FWHM) that varies monitonically from ≈ 1.9 meV at $\epsilon=0$ to ≈ 0.7 meV at $\epsilon=50$ meV. The result of applying these broadenings to the LDA-based calculations gives satisfactory agreement with experiment especially in the high frequency region which is

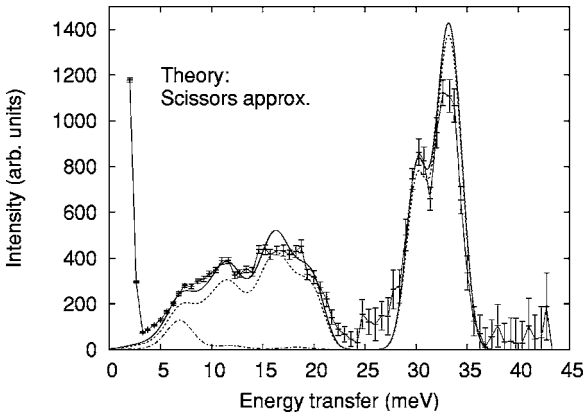

FIG. 5. Theory and experiment for the INS of $La_{0.9}Fe_4Sb_{12}$ corresponding to E_i=50 meV. The experimental results for the 5–9 Å^{-1} Q cut are given, as are the theoretical 5–9 Å^{-1} (solid) and 5–7 Å^{-1} (dashed) Q cuts. The La contribution to the 5–9 Å^{-1} Q cut is also shown. The broadening employed in obtaining the theoretical results includes disorder broadening (see text).

most sensitive to the disorder broadening contribution.

Comparisons with experiment for 5–7 Å^{-1} Q cuts that do not involve the scissors approximation are given in Figs. 6 and 7. Figure 6 also shows the effect of employing disorder broadening. We gain insight into the relation of interatomic forces between filled and unfilled materials through comparisons between the models for $CoSb_3$ and between those models and experiment. It is apparent that model 2 adequately describes the spectrum in the 17–25 meV region which also includes the two calculated A_g frequencies. On the other hand, whereas model 1 yields the same spectral *shape* fairly well, the curves, as well as the calculated A_g frequencies, are shifted to lower frequencies. Upon examining the intrasquare Sb-Sb force constants (see Table II of Ref. 8 and Table I of Ref. 9) we also see that the corresponding values for $CoSb_3$, model 2, are substantially larger than those for $LaFe_4Sb_{12}$. We conclude that these force constants are indeed reduced in the filled materials from their values in the unfilled material.

VI. PARTIAL INS SPECTRA

Consider the following values for the total atomic cross sections: 11.66, 4.2, 2.9, 10.2, and 6.15 barns for Fe, Sb, Ce, La, and Co, respectively. (Our calculations have made use of these values.) The difference between the atomic cross sections of Ce and La were utilized in a previous study[3] to extract the rattling ion contribution. In Fig. 8 we present the theoretically calculated partial contributions to the INS spectra of $La_{0.9}Fe_4Sb_{12}$ for incident neutron energies of 30 meV and 50 meV; the same broadening as for the full spectra was applied. We note that partial spectra for Fe and filler atoms have been directly measured by nuclear inelastic scattering measurements and reasonable agreement with model results was also reported.[5] The number of modes in frequency-separated regions is determined by the number of the corresponding branches of the dispersion curves. Therefore the differences between the integrated intensities of the high frequency peaks of the different materials ought to be directly

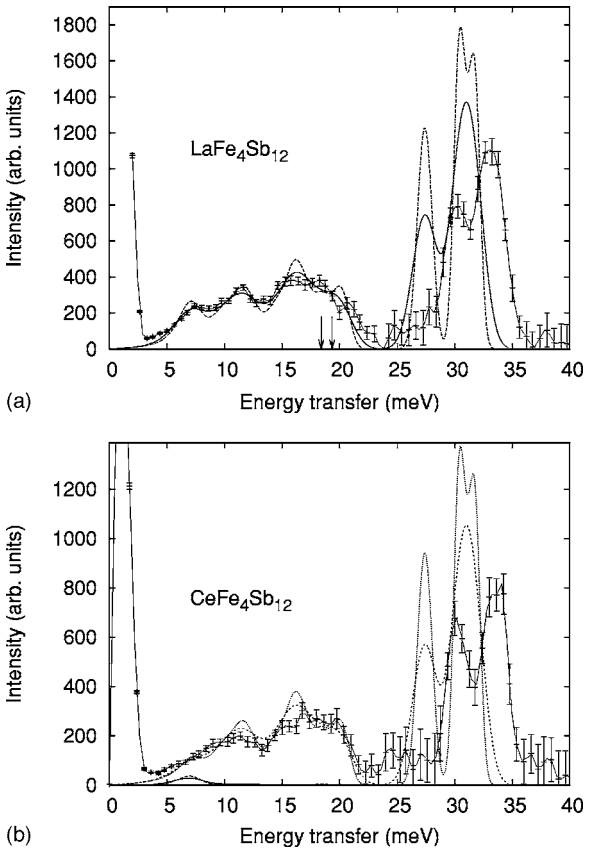

FIG. 6. Theory and experiment for the INS of $La(Ce)_{0.9}Fe_4Sb_{12}$. The two theory curves correspond to theoretical instrumental broadening alone (dotted) and disorder broadening included (dashed). The Ce contribution for $Ce_{0.9}Fe_4Sb_{12}$ is also shown. The arrows correspond to the calculated A_g frequencies.

proportional to the difference in the corresponding TM atomic cross sections. This explains why the Co peak in $CoSb_3$ is seen to be weaker in relation to the rest of the spectrum than is the Fe peak in $La(Ce)Fe_4Sb_{12}$.

VII. VDOS AND PARTIAL VDOS

Figure 9 also shows the VDOS for the three models that we have considered in this paper. Let us first discuss the results for $CoSb_3$. (Note that because we use the Fe mass for model 1 we call this material "$FeSb_3$.") The peak that occurs at about 7 meV for both models 1 and 2 corresponds to the maximum of the transverse acoustic like portion of the spectrum (see the Appendix). It should also be recognized that the slopes, at long wavelengths, of the transverse acoustic (TA) branches along Γ-H reflect the absence of rotational invariance of the force constant model (see the Appendix). Thus perhaps an improvement to model 1 will yield a similarly sharp TA peak to that of model 2. A big difference between models 1 and 2 is also the anomalously sharp peak in the VDOS for model 1. This peak is confirmed by the corresponding feature in the neutron spectrum at ϵ =10 meV (see Fig. 4), and the absence of such a peak for model 2 represents a failure of that model. These results also suggest that the force constants which give rise to these low

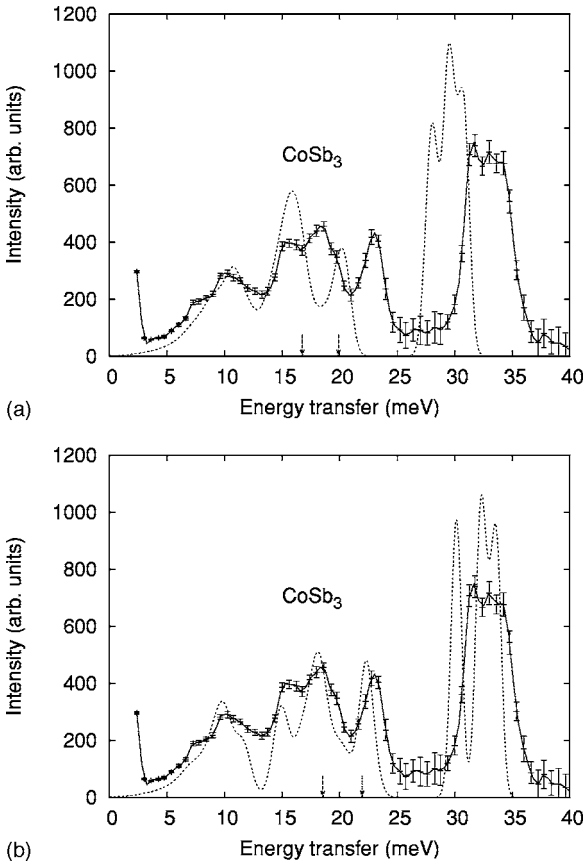

FIG. 7. Theory and experiment for the INS of $CoSb_3$. The theory curve is based on models 1 (upper panel) and 2 (lower panel) (see text). The theoretical instrumental broadening is used. The arrows correspond to the calculated A_g frequencies.

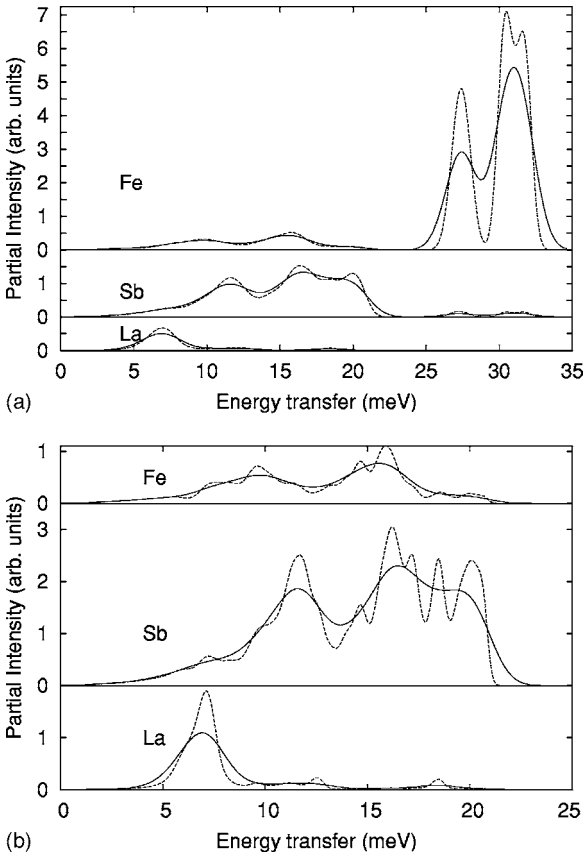

FIG. 8. Partial contributions to the INS of $La_{0.9}Fe_4Sb_{12}$ calculated for $Q=5-7$ Å^{-1} cuts for both $E_i=30$ meV (lower panel) and $E_i=50$ meV (upper panel). The solid lines include disorder broadening and the dashed lines do not (see text).

frequency features, probably the intersquare force constants (see Ref. 14), not change between the filled and unfilled materials. in the neutron spectrum at $\epsilon=10$ meV (see Fig. 4). We note that the analysis performed by Hermann *et al.*[4] for obtaining a rattling ion peak is not possible in our case because of the fact that the La peak occurs in the strongly dispersed region of the $CoSb_3$ spectrum. We have also plotted the partial VDOS in the case of $LaFe_4Sb_{12}$ (Fig. 10), and it is interesting to point out the low frequency side peak in the La partial VDOS. This feature was noticed by Viennois *et al.*,[10] who suggested highly resolved experiments to test the theory. It is due to transverse acoustic-like modes with large La content near the zone boundaries. In particular the low frequency 110 TA branch near N (see the Appendix) contributes to the La partial VDOS. Such a side peak is absent when the Sb mass is replaced by the P mass because in that case the rattling ion frequency falls in the elastic region of the spectrum.

In addition, the (negative) bond-stretching force constant between La and Fe[21] has a measureable, qualtitative, effect on the spectrum. Instead of two separate TM peaks in $CoSb_3$, as in $LaFe_4Sb_{12}$, there is only one. This is understood by considering the nature of the normal modes that contribute to the spectra in the high frequency region. The TM atoms vibrate along the La-TM (or La-void) direction in one peak and perpendicular to it in the other (see Fig. 11).

VIII. COMPARISONS TO RAMAN DATA

Kendziora and co-workers have obtained room temperature results for Raman spectra in both $La_{.75}CoFe_3Sb_{12}$ (Ref. 9) and $CoSb_3$.[13] There are also IR data for $CoSb_3$ as a function of temperature.[14] It is especially interesting to note that for an F_g mode of $CoSb_3$ Kendziora and Nolas obtain 110 cm^{-1} (13.6 meV) whereas our models yielded 98 cm^{-1} (12.2 meV) and 95.6 cm^{-1} (11.9 meV). Figure 4 shows peaks in the INS spectrum corresponding to these zone center modes, and, therefore, a discrepancy between the measured and calculated INS spectra that is consistent with the discrepancy between the calculated and measured Raman frequencies. Furthermore, the Raman spectrum for $La_{.75}CoFe_3Sb_{12}$ is seen to be in quite good overall agreement with the neutron data. The Raman spectrum is sensitive to Sb vibrations and is broadened because of the large amount of disorder. The lowest peak is at 11.5 meV and the intensity goes to zero at about 22 meV consistent with the neutron spectrum. This agreement is quite understandable, since the dispersion is weak in the upper frequency region (see the Appendix). It is interesting to consider the A_g modes, as these can be correlated with features in the observed spectra. The measured A_gs in $CoSb_3$ are 18.9 meV and 22.2 meV and

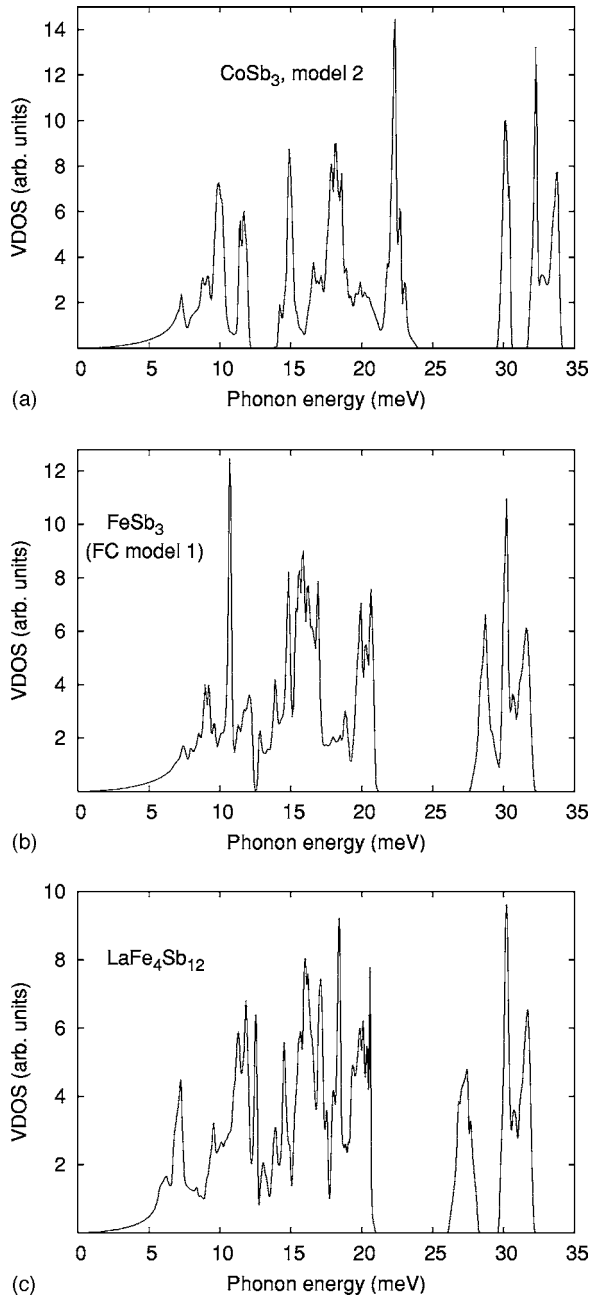

FIG. 9. VDOS for the force constant (FC) models used in this work. In the middle panel the Fe mass is used rather than that of Co in order to provide a direct comparison with the results of the LDA-based calculations for $LaFe_4Sb_{12}$. The comparison shows the effect, in the VDOS, of the La contribution to the FCs (see text).

the predicted values are 16.8 meV and 19.9 meV by model 1. Model 1 therefore predicts the difference between the A_gs rather accurately, but not the absolute values. The different spectral shapes can be explained by the change in δA_g between filled and unfilled materials. In the case of $LaFe_4Sb_{12}$, the results for the A_gs are 18.4 and 19.3 meV. Therefore there exists a much larger difference between the two A_gs in $CoSb_3$ than in $LaFe_4Sb_{12}$, such that one of these A_g modes lies under the new peak formed in the INS spectrum of $CoSb_3$ at approximately 22 meV. Thus perhaps the

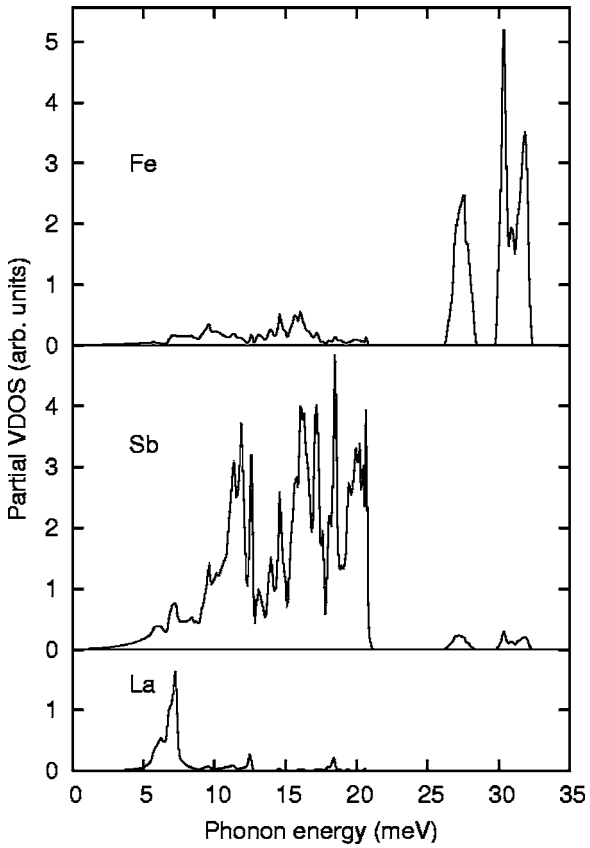

FIG. 10. VDOS contributions for $LaFe_4Sb_{12}$.

A_g frequencies provide a signature of the qualitative changes in the neutron spectrum between filled and unfilled skutterudites.

IX. REANALYSIS OF DATA FOR LA VIBRATIONS

The difference INS spectrum between La- and Ce-filled materials can give information on the La contribution to the density of states because of La's large atomic scattering am-

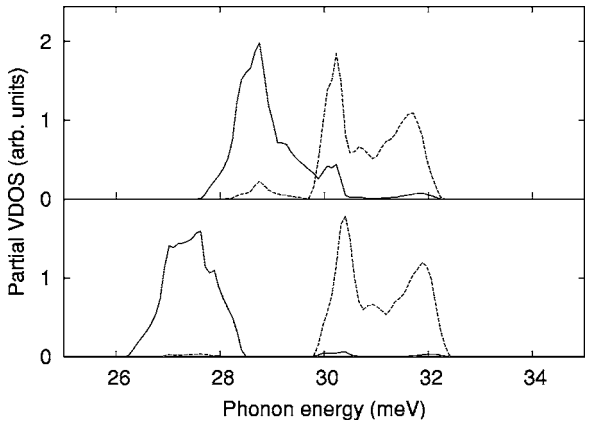

FIG. 11. Fe partial VDOS weighted using components of eigenvectors along parallel (solid) and perpendicular (dashed) directions to the La-Fe "bond" direction. Upper panel corresponds to model 1 for $FeSb_3$ and lower panel to $LaFe_4Sb_{12}$.

plitude in comparison with that of Ce. In addition, results of differences in lattice dynamics between the two materials will be superimposed. Vibrational peaks centered roughly at 7 and 13 meV had been observed in the difference spectrum obtained from experiment, and the 13 meV peak was first interpreted as "extra" lanthanum vibrations[3] but subsequently reinterpreted as lanthanum vibrations due to hybridization with essentially antimony optical modes.[6] The latter interpretation was based on an earlier, less first-principles based, lattice dynamical model than the LDA-based model employed in this work. Recently Viennois *et al.*,[10] who have performed independent neutron scattering measurements on different samples, have stated that our present LDA-based model gives only the lowest frequency (first) peak in the lanthanum weighted VDOS. However, while it is too weak to explain the experimental results, a second-largest peak (and additional higher frequency peaks) due to hybridization with predominantly antimony optical modes, is nevertheless characteristic of the theory (see Fig. 10). Furthermore, recent incoherent nuclear inelastic scattering results[5] have found that the filler atom contributes a strong peak at 7 meV and much weaker higher frequency peaks, in apparent agreement with predictions of the present model. It is important to reconsider the difference spectrum because Viennois *et al.* called into question the existence of the second peak (at 13 meV), and also to compare results for the first peak with those of Viennois *et al.*

In the earlier analysis[3] the difference spectrum was taken from the intensities normalized to one formula unit, and this yielded an unexplained overall larger intensity for the La-filled material than for the Ce-filled material. Here we presume that this overall difference in intensities is simply due to a problem in normalization, such as an uncertainty in the masses of the samples, and we approximately scale the La and Ce results to one another such that the overall positive contribution is eliminated. Thus, before subtracting, we multiply the intensities for the Ce-filled material by 1.3. The results of the subtraction are given in Fig. 12. We point out that although no new measurements were made for the present work, there could be minor differences from the earlier work[3] arising, e.g., from possibly different choices for the energy bins.

The first peak is fitted with a Gaussian and the parameters are given in the figure caption. They compare very well with the values 7.1(1) meV and 4.1(1) meV obtained by Viennois *et al.*[10] for the peak position and breadth (FWHM), respectively. As seen in the figure, our LDA model convoluted with the theoretical instrumental broadening function (curve b) and also (curve a) with a presumed 2 meV broad disorder Gaussian yields a peak that is too narrow peak in comparison with the difference spectrum; a disorder FWHM of 3.3 meV yields much better agreement with experiment.

As seen in Figs. 12 and 10, the second peak in the subtracted data occurs at the same energy as does that of a peak in the LDA-calculated La contribution to the intensity, but the latter is probably too small to be observed in these data. The theoretical result also seems to have been confirmed experimentally by a small second peak, which can unambiguously be identified as arising from vibrations of the filler atom, in nuclear inelastic scattering data.[5] Therefore the second peak in the subtracted neutron data is probably due to the antimony vibrations. In that case, one would expect negative values of intensity differences in neighboring spectral regions (to that of the second peak), and we see from Fig. 12 that this feature is not inconsistent with our measurements. It would be most interesting to investigate these two materials with Raman scattering as that shows only antimony vibrations and hence any differences seen would have to be relegated to lattice dynamics effects. Thus, whereas we confirm that there exists a second peak in the difference spectrum, the origin of that peak is probably not La vibrations.

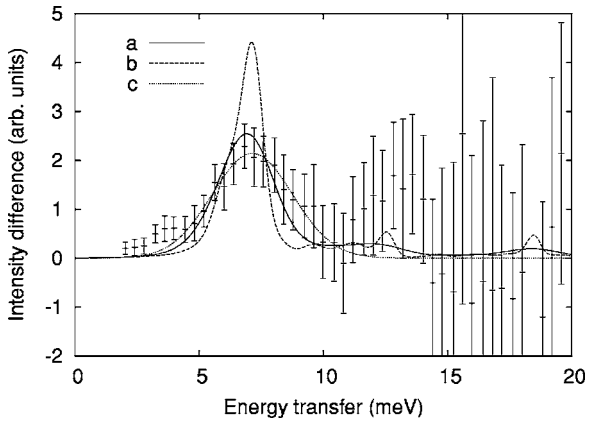

FIG. 12. Difference spectrum for 30 meV incident neutron energies; $La_{0.9}Fe_4Sb_{12}$-$Ce_{0.9}Fe_4Sb_{12}$. The smooth curves show the calculated La partial intensities for two estimates of energy broadening (see text), curves *a* and *b*, and a least square fitted Gaussian function in the 5–10 meV spectral region, curve *c*. The Gaussian parameters for the peak position and breadth (FWHM) are 7.14(7) meV and 3.8(2) meV, respectively.

We also compare values of the "natural" breadth of the first La peak in the difference spectrum for the materials of the two studies. Viennois *et al.*[10] quote an instrumental resolution of 2.4 meV for their measurements. Upon subtraction of the quadratic of their instrumental resolution from that of their measured value of the breadth of the peak we obtain a natural width of 3.3 meV (FWHM) for the Viennois *et al.* experiment. In comparison, we obtain a natural width of 3.7 meV on the basis of the Gaussian fitted parameters given in the Fig. 12 caption and our estimated FWHM $=0.75$ meV instrumental resolution. Other natural widths of filler atom peaks are 2.7 meV for $EuFe_4Sb_{12}$,[5] and 2.3 meV and <0.9 meV for $Tl_{0.8}Co_4Sb_{11}Sn$ and $Tl_{0.8}Co_3FeSb_{12}$, respectively.[4] The FWHM corresponding to the first peak in the La-weighted VDOS for our LDA-based calculations on a perfect crystal is 1.73 meV, which is a very approximate value since the La weighted VDOS does not look much like a Gaussian. It is interesting to speculate that the very small width of <0.9 meV is due to the fact that there is no contribution from zone boundary transverse acoustic modes to the peak in the case of Tl-filled skutterudites. Therefore we have also fitted the La weighted VDOS to a sum of two Gaussians and find that one of the Gaussians—presumably corresponding to the portion of the peak that survives when the Brillouin zone (BZ) boundary TA modes do not contribute—has a 0.5 meV FWHM, which is consistent with the experimental value for $Tl_{0.8}Co_3FeSb_{12}$.

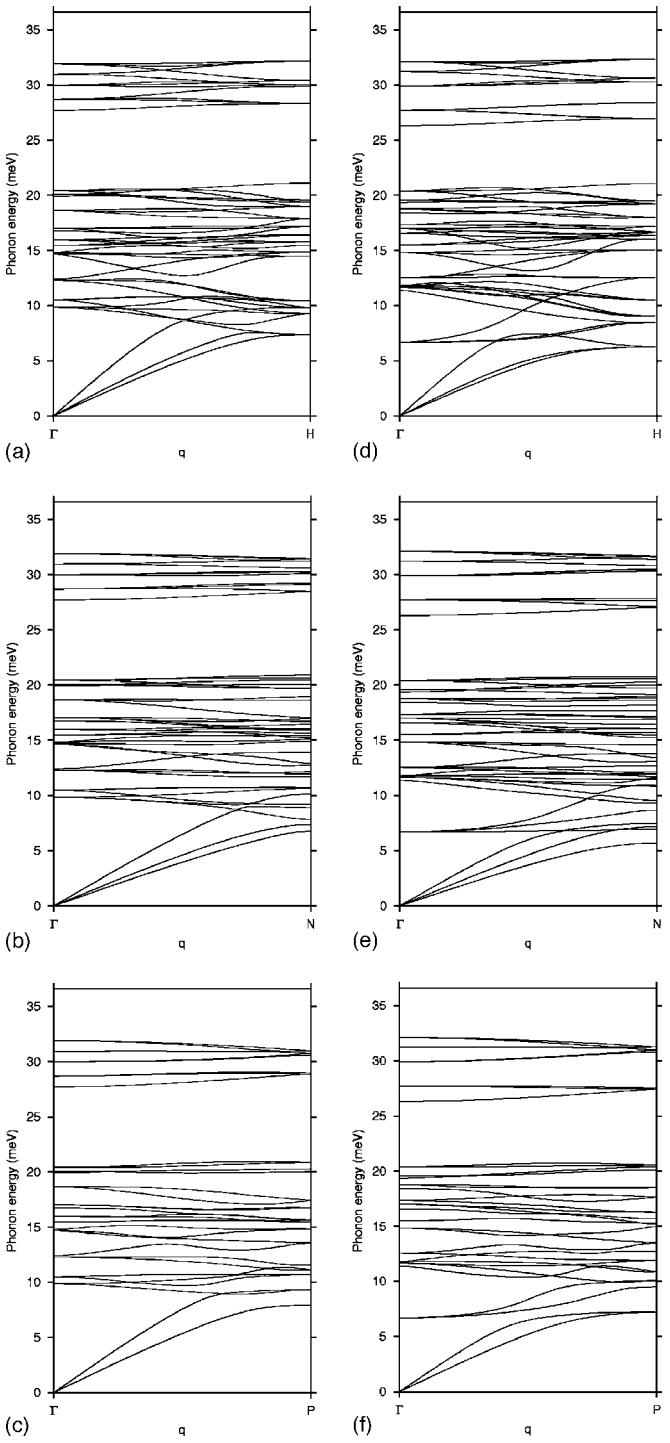

FIG. 13. Dispersion curves along principle directions: Right plots are based on our LDA force constant model for $LaFe_4Sb_{12}$. Left plots are based on that model with the absence of La and small additional force constant changes required by the conservative force condition (see text).

X. CONCLUSIONS

We have presented results for the INS of a few polycrystalline skutterudites and those data have provided a stringent test for lattice dynamical models. An LDA-based short-range tensor force-constant model previously obtained by some of us provided a good description of the spectra of both La-filled and Ce-filled Sb-Fe skutterudites, where the MARI experimental conditions were replicated. Some discrepancies are evident including relative peak heights and reductions of the calculated Fe-dominated peak frequencies in comparison with experiment, but the discrepancies are apparently within LDA accuracy.

Our experimental results also provide a test of a lattice dynamical model for $CoSb_3$ proposed by two of us.[8] We had suggested that there is a 1.5 meV gap in the vibrational spectrum in the 10 to 15 meV region, and a depletion in the density of states in earlier INS measurements taken at Oak Ridge National Laboratory (ORNL), as well as in recent INS measurements,[4] was observed in that region. Supported by the new Raman data[13] and the present INS data, it is now clear that deficiencies in that model gave rise to that prediction. Perhaps there is a gap in the spectrum in this spectral range, but if it exists it must be substantially narrower than 1.5 meV.

We have also seen that the detailed comparison between experiment and theory depends sensitively on the frequency broadening that is used. The results offer the possibility of determining structural disorder broadening.

By comparing data and models for $CoSb_3$ with those of the filled materials it appears that some force constants are similar and some dissimilar between the two types of solids. The process of filling reduces the Sb-Sb bond stretching intra-ring force constants by as much as 30–50%. On the other hand the TM-Sb bonds appear to be virtually unchanged, and apparently the relatively weak, inter-ring, etc., force constants are also similar between the two types of solids; we base the latter conclusion on the ability of the LDA model to reproduce several low frequency spectral peaks for $CoSb_3$.

ACKNOWLEDGMENTS

This work is in part supported by the U.S. Office of Naval Research, NSF DMR-0453804, DOE Nos. DE-FG02-05ER46202 and DE-AC05-00OR22725 with UT/Bettelle LLC (PD). Dr. R. Coldea and Dr. S. M. Bennington were early collaborators on this work and we are grateful to them for their contributions, including many helpful suggestions and development of some of the methods of analysis. We also are grateful to Dr. D. T. Adroja for technical assistance.

APPENDIX

We give the dispersion curves along principal directions for our LDA model with and without La force constants. Note that in the long wavelenth limit the two transverse acoustic branches of the dispersion curves in the Γ-*H* principal direction ought to merge to the same slope by virtue of the cubic symmetry. The reason that there is a small difference in these limiting slopes is that the rotational invariance condition was not imposed on the model[9] and that the symmetry of the structure is not the full 48-cubic-point group symmetry; it does not contain the 90° rotational symmetry.

[1] G. A. Slack and V. G. Tsoukala, J. Appl. Phys. **76**, 1665 (1994).
[2] S. V. Dordevic, N. R. Dilley, E. D. Bauer, D. N. Basov, M. B. Maple, and L. Degiorgi, Phys. Rev. B **60**, 11321 (1999).
[3] V. Keppens, D. Mandrus, B. C. Sales, B. C. Chakoumakos, P. Dai, R. Coldea, M. B. Maple, D. A. Gajewski, E. J. Freeman, and S. Bennington, Nature (London) **395**, 876 (1998).
[4] R. P. Hermann, R. Jin, W. Schweika, F. Grandjean, D. Mandrus, B. C. Sales, and G. J. Long, Phys. Rev. Lett. **90**, 135505 (2003).
[5] G. J. Long, R. P. Hermann, F. Grandjean, E. E. Alp, W. Sturhahn, C. E. Johnson, D. E. Brown, O. Leupold, and R. Rüffer, Phys. Rev. B **71**, 140302(R) (2005).
[6] J. L. Feldman, D. J. Singh, I. I. Mazin, D. Mandrus, and B. C. Sales, Phys. Rev. B **61**, R9209 (2000).
[7] B. C. Sales, D. G. Mandrus, and B. C. Chakoumakos, Semicond. Semimetals **70**, 1 (2001).
[8] J. L. Feldman and D. J. Singh, Phys. Rev. B **53**, 6273 (1996); **54**, 712E (1996).
[9] J. L. Feldman, D. J. Singh, C. Kendziora, D. Mandrus, and B. C. Sales, Phys. Rev. B **68**, 094301 (2003); note that the entry "*xy*" in the third ("5,6") column of values of force constants in Table I should be "−*xy*."
[10] R. Viennois, L. Girard, M. M. Koza, H. Mutka, D. Ravot, F. Terki, S. Charar, and J.-C. Tedanac, Phys. Chem. Chem. Phys. **7**, 1617 (2005).
[11] H. J. Kang, Pengcheng Dai, D. Mandrus, R. Jin, H. A. Mook, D. T. Adroja, S. M. Bennington, S.-H. Lee, and J. W. Lynn, Phys. Rev. B **66**, 064506 (2002).
[12] D. Mandrus, B. C. Sales, V. Keppens, B. C. Chakoumakos, P. Dai, L. A. Boatner, R. K. Williams, J. R. Thompson, T. W. Darling, A. Migliori, M. B. Maple, D. A. Gajewski, E. J. Freeman, Mater. Res. Soc. Symp. Proc. **478**, 199 (1997).
[13] C. A. Kendziora and G. S. Nolas, Mater. Res. Soc. Symp. Proc. **793**, 107 (2004).
[14] H. D. Lutz and G. Kliche, Phys. Status Solidi B **112**, 549 (1982); H. D. Lutz and G. Kliche, Infrared Phys. **24**, 171 (1984).
[15] M. M. Bredov, B. A. Kotov, N. M. Okuneva, V. S. Oskotskii, and A. L. Shakh-Budagov, Sov. Phys. Solid State **9**, 214 (1967).
[16] H. Eschrig, K. Feldmann, K. Hennig, W. John, and L. v. Loyen, Phys. Status Solidi B **58**, K159 (1973).
[17] S. W. Lovesey *Theory of Neutron Scattering from Condensed Matter* (Clarendon Press, Oxford, 1984), Vol. 1.
[18] However, this value differs from that of 2 meV in the caption to Fig. 3 of Ref. 3. It has been suggested (S. M. Bennington, private communication) that the figure caption could be in error. It is also conceivable that there is an inconsistency between the instrumental resolution function determined by the MARI instrumental characteristics and a measurement of the breadth of the elastic line.
[19] J. L. Feldman and D. J. Singh (unpublished).
[20] J. M. Ziman, *Models of Disorder* (Cambridge University Press, Cambridge, England, 1979) p. 366; however, results described herein are not clearly applicable to phonon problems, but see also P. H. Song and D. S. Kim, Phys. Rev. B **54**, R2288 (1996).
[21] J. L. Feldman, D. J. Singh, and I. I. Mazin, *Proceedings of the 18th International Conference on Thermoelectrics, Baltimore, MD* (IEEE, Piscataway, NJ, 1999), p. 9.